*Refereed Proceedings*

*The 12th International Conference on Fluidization - New Horizons in Fluidization Engineering*

Engineering Conferences International *Year* 2007

# In Situ Measurement of Dynamic Mixing in Gas-Solid Fluidized Beds Using Magnetic Resonance

D. J. Holland* P. S. Fennell† C. R. Müller‡
J. S. Dennis** L. F. Gladden†† A. J. Sederman‡‡

*University of Cambridge, djh79@cam.ac.uk
†University of Cambridge, psf20@cam.ac.uk
‡University of Cambridge, cm433@cam.ac.uk
**University of Cambridge, jsd1010@cheng.cam.ac.uk
††University of Cambridge, lfg1@cam.ac.uk
‡‡University of Cambridge, ajs40@cam.ac.uk

# IN SITU MEASUREMENT OF DYNAMIC MIXING IN GAS-SOLID FLUIDIZED BEDS USING MAGNETIC RESONANCE

D.J. Holland, P.S. Fennell, C.R. Müller, J.S. Dennis, L.F. Gladden, A.J. Sederman
Department of Chemical Engineering, University of Cambridge, Pembroke Street, Cambridge CB2 3RA, United Kingdom.

## ABSTRACT

Three magnetic resonance techniques were implemented to study solids mixing in a fluidized bed. Ultra-fast FLASH imaging was utilised to measure the dispersion of a tracer particle in real time. A novel MR sequence for measurement of the time-averaged mixing of solids in a fluidized bed was developed. Finally images of the velocity of solids were obtained to measure directly the pattern of solids flow.

## INTRODUCTION

An understanding of the motion of the particles in granular systems is of critical importance in industrial processing operations, such as fluidized bed drying. However, the motion of granular solids is not well understood, partly owing to the difficulties inherent in studying opaque granular media using optical techniques. Techniques employed to make measurements in the core of a bed have included Magnetic Resonance (MR) (1-4), measurements of electrical resistance (5), positron emission particle tracking (PEPT) (6), electrical capacitance tomography (ECT) (7), and X-radiography (8). MR has the advantage that the signal can be encoded for displacement, as well as position, and can therefore yield complementary information on the motion of granular materials in a single system. Thus, by controlling the experimental set-up it should be possible to measure the motion and dispersion of a tracer particle, as in PEPT, the displacement of particles, as in diffusing wave spectroscopy (DWS) (9), or the total density of particles, as in X-ray and ECT techniques. Furthermore, it is possible to obtain spatially resolved velocity maps, as in Particle Imaging Velocimetry (PIV), giving the flow pattern in a gas-solid fluidized bed. This versatility makes MR unique among three-dimensional tomographic techniques. MR has previously been applied to study the motion and mixing of solids in a variety of granular systems, *e.g*. segregation in rotating cylinders (4), dynamics of vibro-fluidized beds (10) and gas-solid fluidized beds (1-3, 11, 12). In this paper three MR techniques – the FLASH approach, velocity imaging and a novel technique – have been used to study the mixing of solids in a gas-solid fluidized bed. The first technique allows the study of axial segregation and mixing of solids in real time in a 3D fluidized bed, providing a direct comparison with many conventional methods of studying the mixing of solids in a fluidized bed. The last two techniques utilize the ability of MR to label and track particles *in situ* without the need for a tracer, therefore separating mixing from the effects of loading of solids on to the bed. Furthermore, because the "tracer" is the bed material itself, it is possible to repeat the experiment rapidly in order to obtain descriptions of the time-averaged behaviour in a fluidized bed in ~30 minutes. Thus, in the novel MR sequence presented here, the "intrinsic" mixing of solids is examined, while in the velocity

imaging the distribution of the average particle velocities is obtained.
The 12th International Conference on Fluidization - New Horizons in Fluidization Engineering, Art. 61 [2007]

## EXPERIMENTAL

### Apparatus

The fluidized bed (40 ml slumped volume) was contained in an acrylic tube (i.d. 44 mm, o.d. 60 mm) placed vertically within the MR equipment. This gave a bed with a settled depth of ~26 mm. The distributor was a porous glass frit (porosity ~40 %, pore size range 100-160 μm). Dried air was supplied by a compressor and regulated to ~1 bara. The pressure drop across the frit at $U_{mf}$ was between 500 and 2100 Pa, and always greater than the pressure drop across the bed (< 200 Pa).

The oil present in certain seeds is detectable by MR and serves as a means of detecting particles of interest. In this work Myosotis seeds (Suttons Seeds, UK) were used ($T_1$ and $T_2$ relaxation times ~430 ms and ~100 ms respectively); the seeds were 0.9 mm in diameter with an apparent density of 900 kg $m^{-3}$, giving a minimum fluidization velocity ($U_{mf}$) of 0.19 m $s^{-1}$ at ambient conditions. For tracer mixing studies, the bed consisted of suglet particles (NPPharm, 0.55 mm diameter) with an apparent density of 1600 kg $m^{-3}$ giving a $U_{mf}$ of 0.20 m $s^{-1}$ at ambient conditions. Suglet particles are not detectable by MR. In an experiment a 2 ml sample of the Myosotis seeds was dropped on to the surface of a bed of suglet particles using a small hopper situated 30 mm above the bed. The flow of seeds from the hopper took less than 0.1 s. A positioning device was designed such that the seeds from the hopper fell on top of the bed, either near the wall or on the axis of the bed.

### MR Experiments

MR experiments were performed using a Bruker DMX 200 spectrometer operating in the vertical orientation at a proton ($^1$H) frequency of 199.7 MHz. A birdcage radio frequency (r.f.) coil (i.d. 64 mm) situated around the outside of the fluidized bed was used to excite and detect the seeds. The dimensions of the coil constrained the diameter of the column that was employed. Spatial resolution was achieved using a 3-axis shielded gradient system capable of producing a maximum magnetic field gradient of 0.139 T $m^{-1}$.

Three MR techniques were used in this work. The first of these was a conventional FLASH imaging technique (13) and was used to measure the axial distribution of the tracer particles as a function of time. The resolution of these experiments was 625 μm with a repetition time of 11 ms and a tip angle of 0.15 radians. A homospoil gradient of 0.08 T $m^{-1}$ was applied for 300 ms after the acquisition. The second technique consisted of an MR imaging technique where the velocity was encoded in the phase of the observed signal using a sine-shaped velocity encoding gradient (12). This experiment utilised a bed comprising only seeds to produce a time averaged map of the solids motion in the fluidized bed. The spatial resolution in these images was 430 μm × 430 μm; the slice thickness was 5 mm. The sine gradient was applied with a period of 1.1 ms and amplitude of 0.12 T $m^{-1}$. The third technique also measured the mixing of a fluidized bed comprising only seeds using the novel MR sequence shown in Fig. 1. Here, all of the seeds in a defined horizontal slice of the bed were excited. After a delay time, Δ, the axial position of the excited particles was determined by application of a read-gradient. The axial spatial

resolution of this MR experiment was 625 μm; Δ was varied between 25 and 500 ms and 1000 signal averages were acquired giving a total experimental time for a single value of Δ of ~30 minutes. The initial excitation was for a 5 mm thick slice, 22 mm above the distributor. The amplitude of the signal was observed to decay with the $T_1$ relaxation time constant as expected (14). At higher gas velocities, the system will become less stable and the observed MR signal will decrease. The nature of the changes to the signal is the subject of ongoing work.

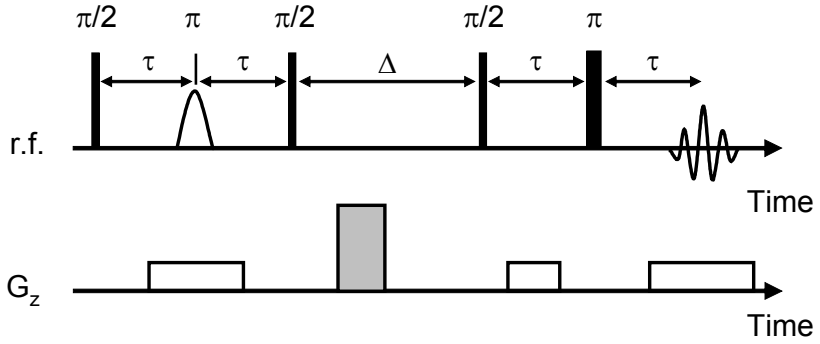


**Figure 1** MR pulse sequence for selective excitation experiments. The first π pulse was a Gaussian excitation to selectively refocus spins at a position fixed by the frequency of the pulse. The shaded gradient was a homospoil pulse.

**Theory**

Two models were applied to the results acquired in this paper. In the one-dimensional Dispersion Model the radial dispersion is assumed to be negligible and the mixing is described by the equation for Fickian diffusion:

$$\frac{\partial C}{\partial t} = D\frac{\partial^2 C}{\partial z^2}. \tag{1}$$

The initial condition for the model was the initial measured distribution of the seeds. It was assumed that the particles travelled around the bed as a discrete bolus of seeds, which dispersed independently of convection about the median of the concentration distribution. Equation (1) was discretised and solved using MATLAB® and the dispersion coefficient was adjusted to minimize the sum of the squared difference between the experimental and simulated tracer distributions. A no-flux boundary condition was used at the top and bottom of the bed.

The second model used was the Counter-Current Back-Mixing (CCBM) model (15) in which the solids were divided into an upwards and a downwards moving phase. The particles in each phase can exchange with the particles in the other phase governed by an exchange parameter, $K_w$. Mathematically, the CCBM model is described by:

$$\frac{\partial C_{up}(z,t)}{\partial t} = -u_{up}\frac{\partial C_{up}}{\partial z} + K_w\left(C_{down} - C_{up}\right) \tag{2}$$

The 12th International Conference on Fluidization - New Horizons in Fluidization Engineering, Art. 61 [2007]

$$\frac{\partial C_{\text{down}}(z,t)}{\partial t} = -u_{\text{down}} \frac{\partial C_{\text{down}}}{\partial z} - K_{\text{w}}\left(C_{\text{down}} - C_{\text{up}}\right) \tag{3}$$

The initial condition for this model was the Gaussian excitation profile defined by the MR experiment. The boundary conditions at the bottom of the bed were:

$$C_{\text{up}}(0,t) = C_{\text{down}}(0,t) \tag{4}$$

$$u_{\text{up}} C_{\text{up}}(0,t) = -u_{\text{down}} C_{\text{down}}(0,t) \tag{5}$$

A similar set of boundary conditions exist at the top of the bed. The CCBM model was solved using the "cinematic" approach (16, 17).

## RESULTS

The results presented in this section cover three areas. Firstly, the results of FLASH experiments using tracer particles are presented and described by the dispersion model. Secondly, the results of the novel imaging sequence involving selective excitation by MR are presented and fitted to the CCBM model. Finally, images of the average velocity of solids in the bed are presented and clearly show the gulf streaming effect.

### FLASH Tracer Studies

Figure 2 shows two intensity profiles of the concentration of seeds loaded on the centre of the top surface at (a) $U/U_{\text{mf}}$ = 1.25 and (b) $U/U_{\text{mf}}$ = 2.0 of a 40 ml bed of suglet particles. It can be seen that the tracer particles in Fig. 2 (a) initially spend some time (~ 1 s) on the top of the bed and then descend and disperse at a fairly uniform velocity down the bed. By the time the tracer particles have reached the bottom of the bed (after 2 -3 s) they are essentially evenly distributed throughout the bed. The striations apparent in the image are due to the motion of bubbles, as described elsewhere (12). There are two key features to note from the axial concentration profiles shown in Fig. 2 (a). Firstly, after the tracer particles were loaded on to the surface of the bed, the mean tracer position dropped to a height of 22 mm above the distributor, before rising again to 32 mm and then dispersing. The mean height of the fluidized bed under these conditions was 29 mm, as can be seen from the concentration profile for times > 3 s. This indicates that the bed temporarily compresses, at least in the vicinity of the tracer particles, for a period of ~100 ms. Secondly, comparing Fig. 2 (a) and (b), it can be seen that there is a pronounced difference between the two experiments. The tracer particles in Fig. 2 (b) clearly descend more rapidly into the bed, but are also seen to rise at about 0.5 s and 1.2 s, presumably as a result of the motion of the bubbles. This behaviour was only observed at $U/U_{\text{mf}}$ = 2.0. However, even at this flow rate it was only observed in four out of 12 experiments and no higher gas flows have been tried. It is also clear from Fig. 2 (b) that the tracer particles disperse more rapidly at $U/U_{\text{mf}}$ = 2.0, as would be expected. In Fig. 2 (a) the particles are evenly dispersed after ~3 s; however, in Fig. 2 (b) the particles are well dispersed after ~1.25 s. At least 6 repetitions of each experiment were performed at the same flow rates and loading position. Significant variations were observed between different repetitions at the same conditions. This apparently random variation in the dispersion process highlights one of the difficulties of studying the mixing of solids in a fluidized bed - it is almost impossible to reproduce exactly the same experimental result. However, by performing several

repetitions it is possible to characterize the mixing of solid tracer particles statistically. This was investigated in an effort to establish how the gas flow rate influences the rate of mixing. The velocity of the downwards moving phase can be estimated from the slope of the mean position of the tracer particle distribution shown in Fig 2. These measurements suggest that the velocity of the downwards moving tracer was 0.4 mm $s^{-1}$, 9 ± 4 mm $s^{-1}$ and 22 ± 9 mm $s^{-1}$ for $U/U_{mf}$ of 0.75, 1.25 and 2.00, respectively. The uncertainty in these measurements was calculated from a 90 % confidence of Student's *t*-distribution of 14 and 12 repeats, respectively; only two repeats were acquired for $U/U_{mf}$ = 0.75 as, visually, no mixing was observed. These values of the velocity of the downflowing solids are comparable with the values of 0, 3 and 25 mm $s^{-1}$ obtained from the correlation of Lim *et al*. (18) with a wake fraction of 0.2. The discrepancy at lower flow rates may be caused by a slight tendency for the particles to segregate.

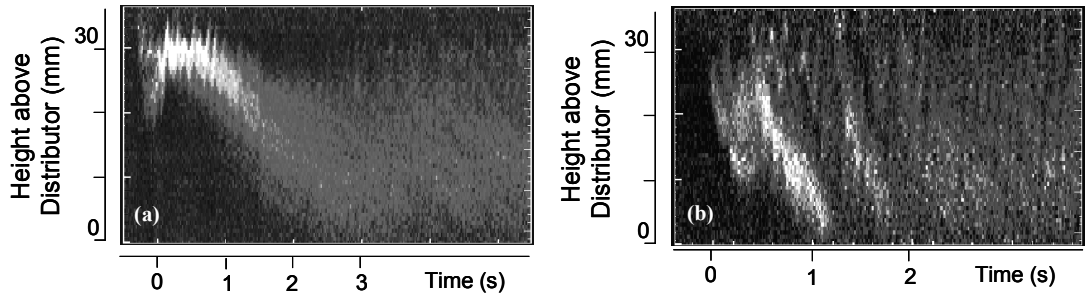


**Figure 2** Two examples of the measured intensity profile of a sample of tracer particles as a function of time. The bright regions correspond to high local tracer concentrations. The gas flow rates were (a) $U/U_{mf}$ = 1.25 and (b) $U/U_{mf}$ = 2.0.

The measurements can be fitted by the dispersion model, which yields dispersion coefficients, *D*, of 2 × $10^{-7}$ $m^2$ $s^{-1}$, (1.0 ± 0.6) × $10^{-5}$ $m^2$ $s^{-1}$ and (4 ± 4) × $10^{-5}$ $m^2$ $s^{-1}$ for superficial gas flow rates of $U/U_{mf}$ = 0.75, 1.25 and 2.00. The uncertainty in these measurements was calculated from the 90 % confidence interval using Student's *t*-distribution with 14 and 12 repeats, respectively. It should also be noted that in all cases where $U/U_{mf}$ > 1 particle mixing was observed. In the case of $U/U_{mf}$ < 1, the dispersion measured is limited by the duration of the experiment. Over the duration of the experiment the change in the distribution of Myosotis seeds amounts to a change in standard deviation of only ~3 %. This is approximately the limit of the accuracy of the measurement. An Analysis of Variance (ANOVA) study was performed on the effect of loading the tracer either near the wall or on the axis of the bed. The ANOVA study revealed with a 90 % confidence that the dispersion coefficient for tracer loaded on to the centre of the bed was greater than that for tracer loaded on to the side of the bed. This is expected, as bubbles more frequently erupt in the centre of the bed than at the wall. Therefore, the tracer loaded on the axis of the bed will be more likely to be scattered over the surface of the bed, or collapse into the void after a bubble eruption. However, FLASH MR is most appropriate for studying mixtures of dissimilar materials, for example in segregation studies. It is not appropriate to study the intrinsic mixing of a fluidized bed. This motivated the development of the selective excitation MR experiment.

The 12th International Conference on Fluidization - New Horizons in Fluidization Engineering, Art. 61 [2007]

**Selective Excitation**

The selective excitation experiment utilised the MR sequence shown in Fig. 1 on a bed containing only Myosotis seeds such that the intrinsic mixing of the solid in a fluidized bed could be measured independently of start-up and loading conditions. An example of how the resulting distribution of the excited seeds varied with time is shown in Fig. 3 for $U/U_{mf}$ = 2.0. The excited seeds were initially located ~22 mm above the distributor, the exact position being determined by the frequency of the Gaussian r.f. pulse. As seen in Fig. 3, the main peak broadens and moves down the column; also a second peak appears with time. The downwards velocity of the main peak can be extracted from the change in its mean position with time. This yields a value of 16 ± 1 mm $s^{-1}$. An effective dispersion coefficient of 8.8 ± 0.1 × $10^{-6}$ $m^2$ $s^{-1}$ can also be obtained from the broadening of this peak as a function of time. However, this dispersion coefficient clearly does not describe the full extent of the mixing of solids in a fluidized bed, as no account is taken of the second peak appearing at the top of the bed. In an effort to justify the appearance of this second peak, the CCBM model was applied to results for $U/U_{mf}$ = 2.0. The simulated concentration profiles are also shown in Fig 3. The simulated profiles are consistent with the experimental profiles, confirming that the appearance of a second peak in the distribution is not unreasonable if both upwards and downwards flowing phases are present in the fluidized bed. The CCBM model has three parameters – the velocity of the downward moving material, the velocity of the upwards moving material and the rate of exchange between the two phases. A least squares fit of the CCBM model to the experimental observation in Fig. 3 (i.e. as obtained from the selective excitation sequence) yields hypothetical velocities of 0.019 m $s^{-1}$ and 0.19 m $s^{-1}$ for the downwards and upwards moving phases, respectively. These values will be compared with direct measurements of the velocity of the solid particles in the next section. The exchange coefficient was found to be ~4 $s^{-1}$. Using the correlation of Darton *et al*. (19) the value of $K_w$ should be ~1 $s^{-1}$, comparable to the best fit value obtained here.

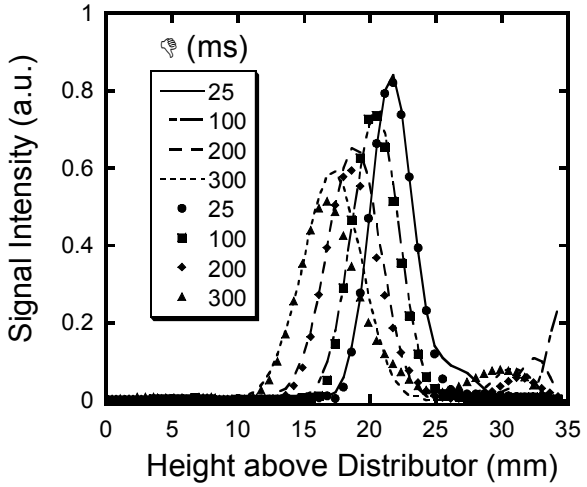


**Figure 3** Plots of signal intensity showing the relative number of excited particles at different heights above the distributor, as measured using the selective excitation MR sequence at $U/U_{mf}$ = 2.0. The excitation position was 22 mm above the distributor. Lines show the best fit of the CCBM model to the measurements. Delay times (Δ) used in the experiment are given in the key.

### Velocity Imaging

Finally, images were acquired of the time-averaged velocity of solids in a fluidized bed using MR. In these experiments the time-averaged velocity of the solids at a given location is proportional to the phase of the signal at that position. Fig. 4 shows a velocity image for a 40 ml bed of particles at $U/U_{mf}$ = 2.0 acquired over a period of ~30 minutes. Fig. 4 clearly shows the Gulf Streaming effect, where particles in the centre of the bed tend to flow upwards and particles at the walls tend to flow downwards. The width of the central upwards moving region increases slight towards the top surface of the bed but is ~18 mm. The region near the distributor shows minimal upwards movement, probably owing to the effect of time-averaging. The time-averaged velocity tends to increase approximately linearly with height. In the radial direction, the velocity is roughly parabolic in the central upwards flowing region and constant in the downwards flowing region. The average velocity of the solids at a height of 20 mm above the distributor in the downwards flowing regions was 0.014 m $s^{-1}$, in reasonable agreement with the values measured using the selective excitation experiment and the best fit of the CCBM model. The velocity of the particles in the upwards flowing regions was between 0 and 0.35 m $s^{-1}$, with a mean value of 0.1 m $s^{-1}$. However, it is important to note that the time-averaged velocity of solids is not constant, but varies with both height and radial position. The positional variation in time-averaged velocity is presumably related to both the frequency at which bubbles pass through different locations and the size of the bubbles in the bed.

## CONCLUSIONS

Three MR techniques have been examined for studying mixing in a gas-solid fluidized bed. FLASH tracer imaging was utilised to measure the dispersion of two types of particle with similar minimum fluidization velocities. These measurements provide a unique method of investigating the mixing of dissimilar particles in real-time in a 3D fluidized bed. A novel MR sequence for measurement of the solid mixing in a gas-solid fluidized bed was developed and implemented. This MR sequence was found to provide a good measure of the time-averaged mixing properties of a gas-solid fluidized bed. The experimentally measured profiles were consistent with a CCBM model incorporating the bulk flow pattern of solids in the bed. Finally velocity images were obtained to measure directly the Gulf Streaming effect in gas-solid fluidized beds.

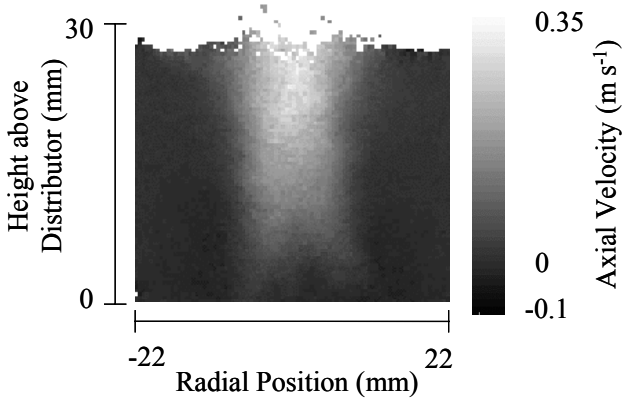


**Figure 4** Image showing the velocity of the solids in a bed of pure Myosotis seeds. No tracer is required and the velocity is recorded in the phase of the measured signal. The image was time-averaged over a period of 30 minutes.

The 12th International Conference on Fluidization - New Horizons in Fluidization Engineering, Art. 61 [2007]

## ACKNOWLEDGEMENT

The authors would like to acknowledge the financial support of EPSRC (EP/C547195/1) and Suttons Seeds Ltd for supplying the seeds.

## NOTATION

$D$ is the dispersion coefficient of the seeds ($m^2\ s^{-1}$), $U$ is the velocity of the gas ($m\ s^{-1}$), $\Delta$ is the delay time in the selective excitation experiments (ms), $C$ is the concentration of tracer particles in the bed (a.u.), $u$ is the velocity of the solids and with subscripts up and down referring to the up-flowing and down-flowing phases ($m\ s^{-1}$), respectively. $U_{mf}$ is the velocity of gas required to just fluidize the particles ($m\ s^{-1}$) and $K_w$ is the wake exchange coefficient ($s^{-1}$).

## REFERENCES

1. P.S. Fennell, J.F. Davidson, J.S. Dennis, L.F. Gladden, A.N. Hayhurst, M.D. Mantle, C.R. Müller, A.C. Rees, S.A. Scott, A.J. Sederman (2005) Chem. Eng. Sci., **60**, 2085.
2. S. Harms, S. Stapf, and B. Blumich (2006) J. Magn. Reson., **178**, 308.
3. R. Savelsberg, D.E. Demco, B. Blumich, S. Stapf (2002) Phys. Rev. E, **65**, 020301.
4. M. Nakagawa, S.A. Altobelli, A. Caprihan, E. Fukushima (1997) Chem. Eng. Sci., **52,** 4423.
5. T. Hayakawa, W. Graham, G.L. Osberg (1964) Canadian J. Chem. Eng., **42**, 99.
6. M. Stein, Y.L. Ding, J.P.K. Seville, D.J. Parker (2000) Chem. Eng. Sci., **55**, 5291.
7. H.S. Tapp, A.J. Peyton, E.K. Kemsley, R.H. Wilson (2003) Sensors and Actuators B-Chemical, **92**, 17.
8. P.N. Rowe, C.X.R. Yacono (1976) Chem. Eng. Sci., **31**, 1179.
9. N. Menon, and D.J. Durian (1997) Phys. Rev. Lett., **79**, 3407.
10. C. Huan, X.Y. Yang, D. Candela, R.W. Mair, R.L. Walsworth (2004) Phys. Rev. E, **69**, 041302.
11. C.R. Müller, J.F. Davidson, J.S. Dennis, P.S. Fennell, L.F. Gladden, A.N. Hayhurst, M.D. Mantle, A.C. Rees, A.J. Sederman (2006) Phys. Rev. Lett., **96**, 154504.
12. A.C. Rees, J.F. Davidson, J.S. Dennis, P.S. Fennell, L.F. Gladden, A.N. Hayhurst, M.D. Mantle, C.R. Müller, A.J. Sederman (2006) Chem. Eng. Sci., **61**, 5702.
13. A. Haase, J. Frahm, D. Matthaei, W. Hanicke, K.D. Merboldt (1986) J. Magn. Reson., **67**, 258.
14. D.J. Holland, C.R. Müller, J.F. Davidson, J.S. Dennis, L.F. Gladden, A.N. Hayhurst, M.D. Mantle, A.J. Sederman, (2007) submitted to J. Magn. Reson.
15. J.J. van Deemter (1985) Mixing, in Fluidization, J.F. Davidson, R. Clift, D. Harrison, Editors. Academic Press: London.
16. C.C. Lakshmanan, and O.E. Potter (1990) Chem. Eng. Sci., **45**, 519.
17. G. Grasa, and J.C. Abanades (2002) Chem. Eng. Sci., **57**, 2791.
18. K.S. Lim, J.Z. Zhu, J.R. Grace (1995) Int. J. Multiphase Flow, **21**, 141.
19. R.C. Darton, J.F. La Nauze, J.F. Davidson, D. Harrison (1977) Trans. Inst. Chem. Eng., **55**, 274.